Combined estimation of thickness and velocities using ultrasound guided waves: a pioneering study on in vitro cortical bone samples

Josquin Foiret, Jean-Gabriel Minonzio, Christine Chappard, Maryline Talmant, Pascal Laugier

Combined estimation of thickness and velocities using ultrasound guided waves: a feasibility study on *in vitro* cortical bone samples

J. Foiret[1,2,3], J.-G. Minonzio[1,2,3], Ch. Chappard[4], M. Talmant[1,2,3], P. Laugier[1,2,3]

[1]Sorbonne Universités, UPMC Univ Paris 06, UMR 7623, Laboratoire d'Imagerie Biomédicale, F-75006, Paris, France
[2]CNRS, UMR 7371, Laboratoire d'Imagerie Biomédicale, F-75006, Paris, France
[3]INSERM, UMR_S 1146, Laboratoire d'Imagerie Biomédicale, F-75006, Paris, France
[4] University Denis Diderot- PRES University Sorbonne Paris Cite, UMR CNRS 7052, B2OA, F-75010, Paris, France

Abstract

In this paper, the issue of the determination of both thickness and elastic characteristics from the propagation of multiple Lamb waves on *ex-vivo* human long cortical bones is addressed. Prior to the measurements on bone, the method is validated on cortical bone-mimicking phantoms. The experimental set-up was previously developed for clinical measurement and the multi-Lamb mode response is analyzed using the singular value decomposition signal processing method recently introduced in the field. The repeatability and the trueness of the estimated parameters on bone-mimicking phantoms were found around a few percent. Estimation of cortical thickness on bone samples was in good agreement with cortical thickness derived from high-resolution peripheral quantitative computed tomography data analysis of the samples.

I. INTRODUCTION

Our domain of interest is bone characterization, *i.e.* determination of structural and material properties by means of ultrasound waves. More precisely, our attention is focused on long cortical bones at peripheral skeletal sites such as tibia or radius. These sites are mainly examined by the use of the so-called axial transmission technique. Emitter(s) and receiver(s) are aligned along the long axis of the bone in contact with the skin (*in vivo*) or directly with the bone specimen (*ex vivo*) using gel as coupling agent. The signals typically transmitted on a distance of a few centimetres are processed to provide the characteristics of the propagation. Using this technique, ultrasound guiding by cortical walls was evidenced in several *ex vivo* measurements and Lamb waves (LW) or their counterpart on curved interfaces were identified [1-5].

Several techniques of bone characterization based on the frequency-dependent characteristics of guided waves, expressed as frequency-wavelength or frequency-velocity relationship were reported. Moilanen *et al.* have exploited a unique branch of the spectrum, the fundamental flexural mode (generally referred as A0 or F11), known to be predominantly sensitive to the waveguide thickness [6-8]. With this method, cortical thickness of 40 human radius specimens was determined using an isotropic hollow tube model for bone. Elastic properties were fixed to tabulated values and the external radius was given. F11 dispersion curve was obtained after selection of its transient response inside the whole multi-component time response. Others studies were based on a multi-mode approach, including higher order modes on bovine samples. Lefevre *et al.* [2] have determined the Young's modulus of two femurs and a tibia using an isotropic plate model for bone, while the thickness and mass density were supposed to be known. Ta *et al.* [9] have estimated cortical thickness of eight tibiae using a tube model from measurements of the three first longitudinal branches. In this latter study, elastic properties were fixed to tabulated values. Multiple modes were resolved

thanks to a time-frequency transform of a unique channel. The same group has also tested a joint approximate diagonalization of eigen-matrices to separate individual components of guided waves. The method was applied to estimate cortical thickness of seven tibiae [10].

All these studies report on techniques for a separate determination of bone thickness or bone elastic properties. However, both thickness and elastic properties participate to bone strength, and we envision that a combined determination of both properties for one individual patient would improve assessment of bone fragility. This assumption takes into account that intracortical porosity is a predominant clinical factor of long bones fragility [11]. Porosity in turn impacts mesoscopic elastic properties of cortical bone and in addition participates to the overall elastic anisotropy of bone as the porous network related to the Haversian system in cortical bone is preferentially orientated along the axis of long bones [12-14]. Thus, the determination of both thickness and cortical mesoscopic anisotropic elastic characteristics from axial transmission measurements can be seen as an intermediate step before further studies focused on porosity and thickness.

Despite the few studies already cited and some others devoted to bone characterization, most of the efforts focus on the experimental protocol and the signal processing. Experimental measurements on bone are challenging, due to the issue of guided waves separation and to the experimental conditions. Irregularities of bone surface or intrinsic properties such as absorption in bone decrease the signal-to-noise ratio compared to laboratory measurements on regular waveguides such as plates and tubes of circular cross section.

In our group, we have adopted a multichannel approach with the advantage of being able to use a compact array adapted to practical clinical measurements. An array for clinical measurements is of reduced length to minimize the impact of the heterogeneity of overlaying soft tissues, in particular their thickness, on the bone ultrasonic response. To resolve multiple modes despite a reduced receiving length, a signal processing based on multichannel response

analysis has been introduced, which takes benefit of the singular value decomposition (SVD) of the bone multichannel response [15]. The signal processing was then adapted to take into account absorbing materials [16]. The current performances of the data acquisition system allowed us to explore the procedure of characterization.

The present paper reports on the reconstruction of both anisotropic elastic characteristic and thickness on five *ex vivo* human radius specimens. The propagation model considered in the following is Lamb wave (LW) propagation in the meridian plane of a transverse isotropic plate. Prior to the application on bone, the method of parameters reconstruction is applied on test case. The test cases focus on several single layers of constant thickness and a tube of circular section, made of a cortical-bone mimicking material. On these test cases, the trueness of the estimation of the elastic parameters was assessed by comparison of the estimates with independent measurements performed using resonant ultrasound spectroscopy [17]. On bone samples, the trueness of the thickness determination was assessed by comparison with the cortical thickness derived from high resolution peripheral quantitative computed tomography measurements (HR-pQCT).

The experimental set-up and the signal processing are reported in Section II. In Section III, the model parameters and the inversion procedure are detailed. Sections IV and V are devoted to results and discussion, respectively.

II. EXPERIMENTAL MEASUREMENTS

A. Samples

Five human radius specimens with overlaying soft tissues removed were investigated. The samples were excised from fresh cadavers. Ethics approval was granted by the Centre du Don des Corps, (Paris, France). The tissue donors provided written consent to provide their tissues for investigation in accordance with legal clauses stated in the French Code of public health.

The specimens were kept frozen before use and gently warmed to room temperature before data acquisition. For each sample, measurements were performed on a standardized region of interest which extends along the length of the receiver array (~2cm) (Fig.1). The center of the probe was placed at around 5.5 cm from the distal end. Measurements were performed on the postero-lateral position.

Controlled measurements were carried out on four single plates of different thickness (1.30 mm, 2.30 mm, 3.35 mm and 4.15 mm) and one tube of circular cross section filled with air with a thickness around 2 mm and external radius of 1 cm. The material of all samples is a composite made of short glass fibers embedded in an epoxy matrix (Sawbones, Pacific Research, MA, USA). The composite material is given as transverse isotropic.

Although cortical bone material and fibers reinforced material are heterogeneous in nature, effective homogenized material properties are investigated by ultrasound waves with wavelengths of millimetric order. At this mesoscopic length scale, the bone material is considered to be transverse isotropic with a plane of isotropy in the transverse cross-section of the long bone. Axes x_1 and x_3 on Fig.1 are supposed to be aligned with the direction of the principal symmetry of the material. The plane (Ox_1x2) is the isotropy plane. The axis x_3 is oriented along the bone axis. Alternatively, in the controlled samples, the axis x_3 is in the fibers direction and the axis x_1 is normal to it.

B. Reference Measurements

Reference measurements were performed independently to the LW measurements to assess the trueness of the LW-based estimation of the sample properties.

First, thickness was assessed on all samples. On plates and tube, thickness was directly measured with a caliper. On bone specimens, the cortical thickness (Ct.Th) of the region of interest measured by ultrasound was assessed using high resolution peripheral quantitative to-

mography (HR-pQCT) with a voxel size of 82 µm (XtremCT (Scanco Medical, Switzerland). Cortical thickness *Ct.Th* was assessed in a 9 mm long area centered on the location of the center of the ultrasound probe. A region of interest (ROI) on tomographic cross-sections corresponding to the transverse extent of the probe was defined by the operator (thick lines on Fig.2). The normal direction of the outer contour (periosteal zone) is locally defined using seven neighboring pixels. The local thickness is evaluated by thresholding the profile of Hounsfield units along the normal. A threshold was set to a constant value, corresponding to half of the maximum value. Cortical thickness *Ct.Th* was then the average of thickness over the ROI and over 110 cross sections corresponding to the reception length.

Secondly, independent measurement of stiffness was available for the bone mimicking phantom. Bernard et al. reported the stiffness coefficients obtained from measurements on a cubic sample extracted from the 4 mm-thick plate using resonant ultrasound spectroscopy (RUS) [17]. The results are gathered in Table 1. The stiffness c_{33}, respectively c_{11}, are related to the pure compression bulk wave in the fibers direction, and respectively in the direction normal to it. The corresponding longitudinal bulk velocities are denoted $V_{L//}$ and $V_{L\perp}$. The stiffness c_{55} is related to the pure shear wave with in plane polarization which propagates along the symmetry axis or normal to it associated with the transverse bulk velocity V_{T}. The relations between the stiffness coefficients, the mass density and the bulk velocities in given directions write:

$$c_{11} = \rho V_{L\perp}^2 \quad (1)$$

$$c_{33} = \rho V_{L//}^2$$

$$c_{55} = \rho V_{T}^2$$

The mass density ρ is equal to 1.64 g.cm^{-3}.

The term c_{13} is the non-diagonal term of the stiffness matrix. Table I shows the stiffness coefficients measured by RUS together with the corresponding bulk wave velocities deduced from Eq 1.

C. Experimental Set-Up

The measurement configuration is depicted on Fig. 1. The linear array of emitters and receivers is aligned along the direction of the fibers. The custom made transducer array of piezo composite elements (Vermon, Tours, France) includes a linear arrangement of several emitters and receivers. This probe has a silicone front face with a thickness of around 2 mm. In the experiments reported here, the probe includes N^{R} = 24 receivers and N^{E} = 5 emitters. The array pitch is 0.8 mm. The minimum emitter-receiver distance is 8 mm. The shape of the individual elements is rectangular with a length (8 mm) which is 10 times larger than the width. Individual elements act as small elements along the width with broad angular beam and as extended elements along the length with straight beam.

During the measurement, each emitter is excited with wideband pulses with a central frequency of 1 MHz (-6 dB power spectrum spanning the frequency range of 0.5 to 1.6 MHz). Signals are recorded at a sampling frequency of 20 MHz (1024 time samples, 12 bits). Before recording, each signal is 16 times averaged by hardware. The driving electronics has been manufactured by Althaïs Technologies (Tours, France).

D. Signal Processing

The multi-channels time series are transformed in the (wavenumber k, frequency f) plane according to the method introduced in [15]. Moreover, this study has taken benefit of the last improvements of the method, which enhances the response of attenuated guided waves [16].

In this study, the attenuation of guided waves originates in visco-elastic absorption in the material.

One cycle of measurements consists in the sequential excitation of each of the N^E emitters and yields $N^E \times N^R$ time series signals. First, the $N^E \times N^R$ time series are Fourier transformed with respect to time and then the singular value decomposition is applied on the frequency series.. Finally, the N^E reception singular vectors denoted $\mathbf{U}_n$ are used to form the so-called *Norm* function

$$Norm(f,k) = \sum_{n=1}^{M} \left| \left\langle \mathbf{U}_n(f) \middle| \mathbf{e}^{test}(k,\alpha) \right\rangle \right|^2 \quad (2)$$

with the testing vector $\boldsymbol{e}^{test}$ being a normalized attenuated plane wave of complex wavenumber $k + i\alpha$. The *Norm* function value ranges from 0 to 1 by construction. On the *Norm* function, physical wavenumbers present in the response of the system exhibit as maxima close to 1. The rank *M*, *i.e*. the number of singular vectors kept to form the *Norm* function, is chosen based on a estimation of the signal-to-noise ratio on the singular value spectrum. The method offers the possibility of tuning two parameters to separate signal from noise: singular values and/or the *Norm* function can be thresholded. The rank of the data matrix is heuristically chosen by the operator and is frequency dependent. The maxima of the *Norm* function are located in the (*f*, *k*) 2D space and give the doublets (f^{exp}, k^{exp}) associated with the experimental guided modes as described in Ref.[15, 16].

In these experiments, the SVD based signal processing was employed with a constant value of attenuation α=0.03 Np/mm as it was observed to provide reasonable enhancement of the *Norm* function. The discretization step was Δf = 5 kHz and Δk = 0.01 rad.mm^{-1}. The threshold applied on the *Norm* function was here chosen to 0.6.

E. Experimental Trajectories

On the example depicted on Fig. 3, one can recognize trajectories represented by the maxima of the *Norm* function. These groups of couples (f_{exp}, k_{exp}) are classified and regrouped in N distinct experimental trajectories following the apparition order in function of the frequency. Actually, measurements on laboratory samples (plates and tube) brought evidence that the probe did perturb the measurements. Our analysis suggested that the front face of the probe couples the guided waves in the sample. These operational conditions required the operator to manually reject the most perturbed experimental data. Among the data rejected, the lowest phase velocities (associated to the highest wavenumbers) and data close to the branching locations were withdrawn. An illustration is given by the comparison of Fig. 3 which shows the Norm function and Fig.4 a. on which crosses represent the selected trajectories for the same sample (1.30 mm-thick plate).

After the grouping of raw data into experimental trajectories, each trajectory is associated to a specific Lamb branch numbered n. Lamb branches show up as piecewise curves as some frequency regions are not observed. This effect is related to insufficient out-of-plane displacement and to a high attenuation due to absorption in the material. To reduce the ambiguity on the link between an individual Lamb branch and a given experimental trajectory, a bank of calculated Lamb spectrum was compared to the experimental data. The choice is made on the basis of a reasonable agreement of the overall pattern (number of branches, trend of frequency-dependent wavenumber) of both data. To feed the bank of calculated spectrum, a reference mean elastic model is used (Table 1) [18] and the unique effect of thickness variation is considered. We are particularly interested in cases with large inter-samples changes in thickness and moderate inter-samples changes in elastic properties which is a reasonable assumption for cortical bone.

III. PARAMETERS IDENTIFICATION

A. *Parameters*

Solutions of the Lamb wave dispersion equation are frequencies f obtained as function of given values of wavenumber k and, for propagation in the meridian plane, they appear as determined by prescribed thickness, mass density and stiffness c_{11}, c_{33}, c_{13}, c_{55}, as reported in [19, 20]. In the field of non destructive testing, for anisotropic single layers, the search of absolute elastic moduli (stiffness) has been the focus of several previous investigations, and this requires prescribing the mass density and the thickness [21-25]. In the field of bone characterization, within the framework of clinical measurements, (excluding biopsy), the mass density cannot be known independently. In addition the mass density is subjected to inter-individual variability for instance under the effect of the variability of intracortical porosity [11]. The difficulty is overcome by formulating the dispersion equation as function of phase velocities of the bulk wave, the mass density is then embedded in velocity parameters.

Alternatively, Lamb wave equations can be formulated with one bulk wave velocity in a particular direction and three stiffness ratios (see Appendix). The pure shear wave velocity V_T in the direction of the fibers (Ox_3) is chosen which writes as (Eq 1). The three stiffness ratios c_{13}/c_{11}, c_{11}/c_{55}, c_{33}/c_{11} are considered and the ratio e/V_T was preferentially used. In conclusion, the set of 5 plate parameters is (V_T , c_{13}/c_{11}, c_{11}/c_{55}, c_{33}/c_{11} , e/V_T).

B. *Identification Process*

Reconstruction of elastic properties and thickness is carried out by minimizing the error function χ defined as the square differences between experimental and calculated frequencies f^{exp} and f^{calc}:

$$\chi = \sum_{n=1}^{N} \sum_{i} \left(f_n^{\exp}\left(k_i^{\exp}\right) - f_n^{calc}\left(k_i^{\exp}\right)\right)^2 \quad (3)$$

where the subscript n refers to the experimental trajectories and i to the number of experimental points in the trajectory n. In Eq. 3, f^{exp} and f^{calc} belong to the same trajectory n supposed to be pre-determined as a Lamb branch S_k or A_l.

The optimization is achieved with a gradient method using the inbuilt trust region reflective algorithm for non-linear minimization from Matlab (The MathWorks Inc., Natick, MA) using Optimization Toolbox 6.0. The parameters are restricted to certain limits by specifying simple bound constraints to the constrained optimizer function. Initial guesses were allowed to take random values in pre-defined intervals: [0.5-2.5] (µs) for e/V_T , [1.0-2.0] (mm.µs^{-1}) for V_T , [0.2-0.7] for c_{13}/c_{11}, [1.1-2.5] for c_{33}/c_{11} and [2.5-3.9] for c_{11}/c_{55}. Note that these intervals are rather large. The convergence to a unique solution was checked by running optimization process several times successively with new initial guess values.

IV. RESULTS

First, results on plates and tube are presented. Fig. 4 shows experimental trajectories obtained for the four plates and for the tube. For all five initial guess, parameters converged individually towards the same value as illustrated by Fig. 5 for the 1.30 mm plate. The number of iterations increased with the plate thickness.

In Table 2, the estimated thickness is compared to the reference thickness. Calliper measurements vary typically within 0.02 mm in the area of measurements. Note that the variability of the estimated thickness is also at most 0.02 mm. The relative error on thickness was lower than 2.5 %.

The repeatability and the trueness of the estimated material properties were explored. The bulk waves velocities normal and parallel to the fibers are depicted on Fig 6. These values are deduced from optimized parameters using the relations:

$$V_{L\perp} = V_T \sqrt{\frac{c_{11}}{c_{55}}} \quad ; \quad V_{L//} = V_T \sqrt{\frac{c_{33}}{c_{11}} \frac{c_{11}}{c_{55}}} \quad ; \qquad (15)$$

The intra-sample repeatability is calculated as the half-range divided by the median value over 30 measurements (3 repositioning and 10 measurements by position). The intra-sample repeatability is better than 10 m/s for V_T (<1%), better than 70 m/s for $V_{L\perp}$ (<2.5%), better than 50 m/s for $V_{L//}$ (<1.5%) and better than 0.03 for the ratio c_{13}/c_{11} (<7%),. The 2.30 mm-thick plate presents a repeatability two times worst than the other samples. The inter-sample repeatability is better than 20 m/s for V_T (<1.5%), better than 90 m/s for $V_{L\perp}$ (<3%), better than 110 m/s for $V_{L//}$ (3%) and better than 0.03 for the ratio c_{13}/c_{11} (<7%),.

Estimated velocities are compared to RUS-based velocities obtained on the 4 mm thick plate. Estimated velocities are consistent with the RUS-based velocities: over all plates and tube, differences are inferior to 1.3 % for V_T (around 20 m/s), inferior to 3% for $V_{L\perp}$ (around 90 m/s) and inferior to 2% for $V_{L//}$ (around 70 m/s).

Examination of the goodness-of-fit on Fig. 4, where experimental observations are superimposed to best-fit curves calculated with optimized parameters, indicates an overall good agreement for the 4 plate samples.

Measurements on the tube were intended to investigate the effect of a non flat surface of contact on the results. Measurements on the tube did not reveal any flexural type waves, associated to both tangential and radial particle displacement, but only longitudinal waves with radial displacement. As illustrated on Fig. 4 and Fig. 6, measurements on tube of circular cross section did not degrade the determination of thickness and elastic characteristics.

For the measurements on bone specimens, an overall decrease of the signal-to-noise ratio was observed. For four samples over five, it was needed to smooth the experimental raw data in order to use them as input in the optimization algorithm. Experiments together with the best fits are shown on Figure 7. In this feasibility study, the repeatability was not assessed. Table 3

gives the values of the estimated bulk wave velocities and the estimated thickness as well as the cortical thickness derived from HR-pQCT analysis. Thickness values obtained with the optimization method follow the same trend as the ones measured with HR-pQCT. Table 3 indicates an overall agreement on thickness determination within few hundred microns. Inter-sample variability of bulk wave velocities was higher for $V_{L\perp}$ (14%) than for $V_{L//}$ (around 3%) and for V_T (around 8 %). An overall agreement is obtained with studies on human bones based on transverse transmission of ultrasound bulk waves through small samples extracted from specimen reported in [12, 26, 27]. For example, according to the details of the measurements on human femurs tabulated in [26], bulk wave velocities measured from Lamb wave propagation human radius are consistent with the bulk wave velocities measured on human femur. In this study, V_T was within 1788-1828 m/s depending on which site (postero-medial-anterior or lateral) it was measured, while the $V_{L\perp}$ was between 2715-3066 m/s and $V_{L//}$ was between 3750-3842 m/s.

V. DISCUSSION AND CONCLUSION

In this study, we report on a feasibility test for the combined determination of cortical thickness and elastic characteristics on bone sample from the frequency-dependent properties of Lamb waves. The method was first assessed on controlled samples with simple shape. The identification process uses as parameters one bulk wave velocity, three stiffness ratios and a parameter related to thickness, without the need of determination of the mass density.

Our present approach has several limitations which will be addressed in the future. Five parameters are needed and this relatively high number of unknowns is a cause of uncertainty and inaccuracy of the identification process. The departure from the ideal model which assumes a perfect transverse isotropy, a perfect alignment of the probe on the principal axis as well as a non absorbing material also impact the accuracy. Another likely limitation, related to

the current technology of the front cover of the prototype probe, was noticed as a parasitic effect which smears the experimental data. Another weakness relates to the assignment of a Lamb branch to each experimental trajectory, prior to the parameters optimization. Semi-automatic selection and classification of the experimental trajectories were heuristically done, with the help of prescribed approximate material properties. Improvements are expected from further studies. In the perspective of clinical measurements, further studies will take into account the bidirectional method which allows to correct for the bias on wavenumber measurements related to uneven soft tissue thickness in the region of measurements [28]

Despite these error sources, trueness of thickness and material properties and repeatability were within few percents on controlled samples. Repetitive measurements without and with repositioning help to draw the uncertainties of the estimates met in the experiments. Trueness was evaluated with comparison to RUS measurements, whose results were available for one of the controlled samples investigated in this study. RUS method was also successful in investigating cortical bone samples [29] and thus, future face-to-face comparison between guided waves characterization of bone specimens and RUS estimation constitutes one of the next step of this study.

This study allowed to establish that the human radius sustains the propagation of Lamb waves of higher order: A_1, S_1, S_2 *and* A_3 were identified through the optimization procedure. A second main outcome of the study is the proof of feasibility of the combined reconstruction of material properties and thickness from Lamb waves measurements, using a compact array and SVD based signal processing. The method was applied on ex vivo radius and participates to the main study which is the development of methods dedicated to *in vivo* bone characterization.

Appendix : Dispersion equation

Lamb wave dispersion equation in the meridian plane relates the angular frequency ω, and the wavenumber component k_3 and involves 6 parameters: the plate thickness e, the mass density ρ, and the stiffness c_{11}, c_{33}, c_{13} and c_{55} of the transverse isotropic material [19, 20]. Alternatively, the parameters set $P=\{V_T\ ,\ c_{13}/c_{11},\ c_{11}/c_{55},\ c_{33}/c_{11}\ \}$ is adopted to formulate the equation, where V_T is the velocity of the pure shear wave in the longitudinal and transverse direction and is defined by:

$$V_T = \sqrt{\frac{c_{55}}{\rho}} \quad ; \qquad \text{(A1)}$$

The wavenumber component k_3 and $k_1^{QS,QL}$ verify:

$$\left(k_1^{QS,QL}\right)^2 = \frac{-\Sigma \pm \left(\Sigma^2 - 4\Pi\right)^{1/2}}{2} k_3^{\,2}\,, \qquad \text{(A1)}$$

where the sign + relates to quasi shear (QS) wave. Likewise, the sign $-$ relates to quasi longitudinal (QL) wave. The index 1 and 3 relates to the axis (Ox_1) and (Ox_3) shown in Figure 1. The terms Σ and Π are:

$$\Sigma = \frac{c_{33}}{c_{11}}\frac{c_{11}}{c_{55}} - 2\frac{c_{13}}{c_{11}} - \left(\frac{c_{13}}{c_{11}}\right)^2 \frac{c_{11}}{c_{55}} - \frac{\omega^2}{V_T^2}\frac{1}{k_3^2}\left[1 + \left(\frac{c_{11}}{c_{55}}\right)^{-1}\right]$$

$$\Pi = \left(\frac{c_{11}}{c_{55}}\right)^{-1}\left(\frac{\omega^2}{V_T^2}\frac{1}{k_3^2} - \frac{c_{33}}{c_{11}}\frac{c_{11}}{c_{55}}\right)\left(\frac{\omega^2}{V_T^2}\frac{1}{k_3^{\,2}} - 1\right), \qquad \text{(A2)}$$

Following equations (32) and (34) of reference [29], the dispersion equation of the symmetric Lamb modes S_n can be written as

$$F_S = B_{QS}\sin(k_1^{QS}\,e/2)\cos(k_1^{QL}\,e/2) - B_{QL}\sin(k_1^{QL}\,e/2)\cos(k_1^{QS}\,e/2)\,, \qquad \text{(A3a)}$$

The dispersion equation for the anti-symmetric modes A_n is obtained by inverting the QS and QL upperscripts inside the parentheses in (A3a)

$$F_A = B_{QS}\sin(k_1^{QL}\, e/2)\cos(k_1^{QS}\, e/2) - B_{QL}\sin(k_1^{QS}\, e/2)\cos(k_1^{QL}\, e/2)\,, \qquad \text{(A3b)}$$

The terms $B_{QS,QL}$, and $R_{QS,QL}$ are given by:

$$B_{QS,QL} = (R_{QS,QL}k_3 + k_1^{QS,QL})(R_{QL,QS}k_1^{QL,QS} + \frac{c_{13}}{c_{11}}k_3)$$

$$R_{QS,QL} = \frac{\left[\frac{\omega^2}{V_T} - \frac{c_{33}}{c_{11}}\frac{c_{11}}{c_{55}}k_3^2 - (k_1^{QS,QL})^2\right]}{\left(1 + \frac{c_{13}}{c_{11}}\frac{c_{11}}{c_{55}}\right)k_3 k_1^{QS,QL}} \qquad \text{(A4)}$$

REFERENCES

[1] P. H. F. Nicholson, P. Moilanen, T. Karkkainen, J. Timonen, and S. L. Cheng, "Guided ultrasonic waves in long bones: modelling, experiment and in vivo application," *Physiological Measurement*, vol. 23, pp. 755-768, 2002.

[2] F. Lefebvre, Y. Deblock, P. Campistron, D. Ahite, and J. J. Fabre, "Development of a new ultrasonic technique for bone and biomaterials in vitro characterization," *Journal of Biomedical Materials Research*, vol. 63, pp. 441-446, 2002.

[3] A. Tatarinov, N. Sarvazyan, and A. Sarvazyan, "Use of multiple acoustic wave modes for assessment of long bones: Model study," *Ultrasonics*, vol. 43, pp. 672-680, 2005.

[4] V. C. Protopappas, D. I. Fotiadis, and K. N. Malizos, "Guided ultrasound wave propagation in intact and healing long bones," *Ultrasound in Medicine and Biology*, vol. 32, pp. 693-708, 2006.

[5] D. A. Ta, K. Huang, W. Q. Wang, Y. Y. Wang, and L. H. Le, "Identification and analysis of multimode guided waves in tibia cortical bone," *Ultrasonics*, vol. 44, pp. E279-E284, 2006.

[6] P. Moilanen, V. Kilappa, P. H. F. Nicholson, J. Timonen, and S. L. Cheng, "Thickness sensitivity of ultrasound velocity in long bone phantoms," *Ultrasound in Medicine and Biology*, vol. 30, pp. 1517-1521, 2004.

[7] P. Moilanen, P. H. F. Nicholson, V. Kilappa, S. L. Cheng, and J. Timonen, "Assessment of the cortical bone thickness using ultrasonic guided waves: Modelling and in vitro study," *Ultrasound in Medicine and Biology*, vol. 33, pp. 254-262, 2007.

[8] V. Kilappa, K. L. Xu, P. Moilanen, E. Heikkola, D. A. Ta, and J. Timonen, "Assessment of the Fundamental Flexural Guided Wave in Cortical Bone by an Ultrasonic Axial-Transmission Array Transducer," *Ultrasound in Medicine and Biology*, vol. 39, pp. 1223-1232, 2013.

[9] D. Ta, W. Q. Wang, Y. Y. Wang, L. H. Le, and Y. Q. Zhou, "Measurement of the Dispersion and Attenuation of Cylindrical Ultrasonic Guided Waves in Long Bone," *Ultrasound in Medicine and Biology*, vol. 35, pp. 641-652, 2009.

[10] X. Song, D. Ta, and W. Wang, "Analysis of Superimposed Ultrasonic Guided Waves in Long Bones by the Joint Approximate Diagonalization of Eigen-matrices Algorithm," *Ultrasound in Medicine and Biology*, vol. 37, pp. 1704-1713, 2011.

[11] R. M. D. Zebaze, A. Ghasem-Zadeh, A. Bohte, S. Iuliano-Burns, M. Mirams, R. I. Price, E. J. Mackie, and E. Seeman, "Intracortical remodelling and porosity in the distal radius and post-mortem femurs of women: a cross-sectional study," *Lancet*, vol. 375, pp. 1729-1736, 2010.

[12] M. Granke, Q. Grimal, A. Saïed, P. Nauleau, F. Peyrin, and P. Laugier, "Change in porosity is the major determinant of the variation of cortical bone elasticity at the millimeter scale in aged women," *Bone*, vol. 49, pp. 1020–1026, 2011.

[13] C. Baron, M. Talmant, and P. Laugier, "Effect of porosity on effective diagonal stiffness coefficients (c(ii)) and elastic anisotropy of cortical bone at 1 MHz: A finite-difference time domain study," *Journal of the Acoustical Society of America*, vol. 122, pp. 1810-1817, 2007.

[14] X. N. Dong and X. E. Guo, "The dependence of transversely isotropic elasticity of human femoral cortical bone on porosity," *Journal of Biomechanics*, vol. 37, pp. 1281-1287, 2004.

[15] J. G. Minonzio, M. Talmant, and P. Laugier, "Guided wave phase velocity measurement using multi-emitter and multi-receiver arrays in the axial transmission configuration," *Journal of the Acoustical Society of America*, vol. 127, pp. 2913-2919, 2010.

[16] J. G. Minonzio, J. Foiret, M. Talmant, and P. Laugier, "Impact of attenuation on guided mode wavenumber measurement in axial transmission on bone mimicking plates " *J. Acoust. Soc. Am.*, vol. 130, pp. 3574-3582, 2011.

[17] S. Bernard, Q. Grimal, S. Haupert, and P. Laugier, "Assessment of anisotropic elasticity of small bone samples with resonant ultrasound spectroscopy: attenuation does not prevent the measurements," in *2011 Ieee International Ultrasonics Symposium*, pp. 1599-1602.

[18] **E. Bossy, M. Talmant, and P. Laugier, "Three-dimensional simulations of ultrasonic axial transmission velocity measurement on cortical bone models," *The Journal of the Acoustical Society of America*, vol. 115, pp. 2314-2324, 2004.**

[19] **V. Dayal and V. K. Kinra, "Leaky Lamb Waves in an Anisotropic Plate .1. an Exact Solution and Experiments," *Journal of the Acoustical Society of America*, vol. 85, pp. 2268-2276, 1989.**

[20] **S. H. Rhee, J. K. Lee, and J. J. Lee, "The group velocity variation of Lamb wave in fiber reinforced composite plate," *Ultrasonics*, vol. 47, pp. 55-63, 2007.**

[21] **M. R. Karim, A. K. Mal, and Y. Barcohen, "Inversion of Leaky Lamb Wave Data by Simplex Algorithm," *Journal of the Acoustical Society of America*, vol. 88, pp. 482-491, 1990.**

[22] **D. Fei, D. E. Chimenti, and S. V. Teles, "Material property estimation in thin plates using focused, synthetic-aperture acoustic beams," *Journal of the Acoustical Society of America*, vol. 113, pp. 2599-2610, 2003.**

[23] **P. Puthillath, C. V. Krishnamurthy, and K. Balasubramaniam, "Hybrid inversion of elastic moduli of composite plates from ultrasonic transmission spectra using PVDF plane wave sensor," *Composites Part B-Engineering*, vol. 41, pp. 8-16, 2010.**

[24] **J. Vishnuvardhan, C. V. Krishnamurthy, and K. Balasubramaniam, "Blind inversion method using Lamb waves for the complete elastic property characterization of anisotropic plates," *Journal of the Acoustical Society of America*, vol. 125, pp. 761-771, 2009.**

[25] **S. Dahmen, H. Ketata, M. H. Ben Ghozlen, and B. Hosten, "Elastic constants measurement of anisotropic Olivier wood plates using air-coupled transducers generated Lamb wave and ultrasonic bulk wave," *Ultrasonics*, vol. 50, pp. 502-507, 2010.**

[26] **A. A. E. Orias, J. M. Deuerling, M. D. Landrigan, J. E. Renaud, and R. K. Roeder, "Anatomic variation in the elastic anisotropy of cortical bone tissue in the human femur," *Journal of the Mechanical Behavior of Biomedical Materials*, vol. 2, pp. 255-263, 2009.**

[27] **S. Bensamoun, M. C. H. Tho, S. Luu, J. M. Gherbezza, and J. F. de Belleval, "Spatial distribution of acoustic and elastic properties of human femoral cortical bone," *Journal of Biomechanics*, vol. 37, pp. 503-510, 2004.**

[28] **L. Moreau, J.-G. Minonzio, J. Foiret, E. Bossy, M. Talmant, and P. Laugier, "Accurate measurement of guided modes in a plate using a bidirectional approach," *The Journal of the Acoustical Society of America*, vol. 135, pp. EL15-EL21.**

[29] **S. Bernard, Q. Grimal, and P. Laugier, "Accurate measurement of cortical bone elasticity tensor with resonant ultrasound spectroscopy," *Journal of the Mechanical Behavior of Biomedical Materials*, vol. 18, pp. 12-19.**

List of Tables

Table 1:

Stiffness coefficients and bulk wave velocities. First line: RUS measurements of the bone mimicking material from Ref [17] ; second line: reference mean elastic model used for bone samples [18]

Table 2

Plates and tube. Reference thickness e_{Ref} and LW-based determination of thickness.

Table 3

Bone specimens. Reference thickness ($Ct.Th_{ref}$) and LW-based estimation of cortical thickness ($Ct.Th$). Optimized bulk wave velocities V_T, $V_{L\perp}$ and $V_{L//}$ and optimized anisotropy ratio c_{13}/c_{11} .

Table 1

	Stiffness (Gpa)				Mass density	Velocity ($mm.\mu s^{-1}$)		
	c_{55}	c_{13}	c_{11}	c_{33}	ρ	V_T	$V_{L\perp}$	$V_{L//}$
Phantom [17]	4.3	6.9	13.9	20.9	1.64	1.62	2.91	3.57
Bone mean material [18]	6	11.5	21.5	29.6	1.85	1.8	3.41	4.0

Table 2

e_{ref} (mm)	e (mm)
1.30 ± 0.01	1.28 ± 0.01
2.30 ± 0.02	2.35 ± 0.02
3.35 ± 0.02	3.28 ± 0.01
4.15 ± 0.02	4.10 ± 0.01
Tube : 1.95 ± 0.02	1.94 ± 0.02

Table 3

ID	$Ct.Th_{ref}$ (mm)	$Ct.Th$ (mm)	c_{13}/c_{11}	V_T (mm.µs^{-1})	$V_{L\perp}$ mm.µs^{-1})	$V_{L//}$ (mm.µs^{-1})
1	1.1 ± 0.2	1.0	0.55	1.68	2.70	3.84
2	1.5 ± 0.2	1.4	0.53	1.55	2.57	4.01
3	1.5 ± 0.3	1.6	0.41	1.86	3.49	4.13
4	1.7 ± 0.3	1.7	0.49	1.82	3.25	3.96
5	2.7 ± 0.3	2.7	0.40	1.91	3.50	3.87

List of figures

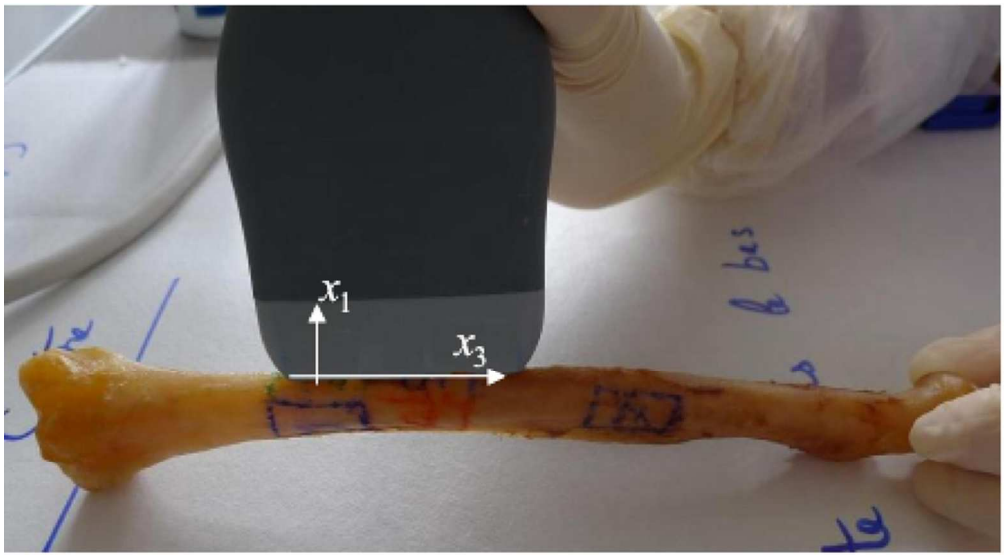

Fig. 1: Measurement configuration with the multi-emitter/multi-receiver probe. Axis x3 is orientated along the bone axis or along the fibers in the bone mimicking plate
86x47mm (300 x 300 DPI)

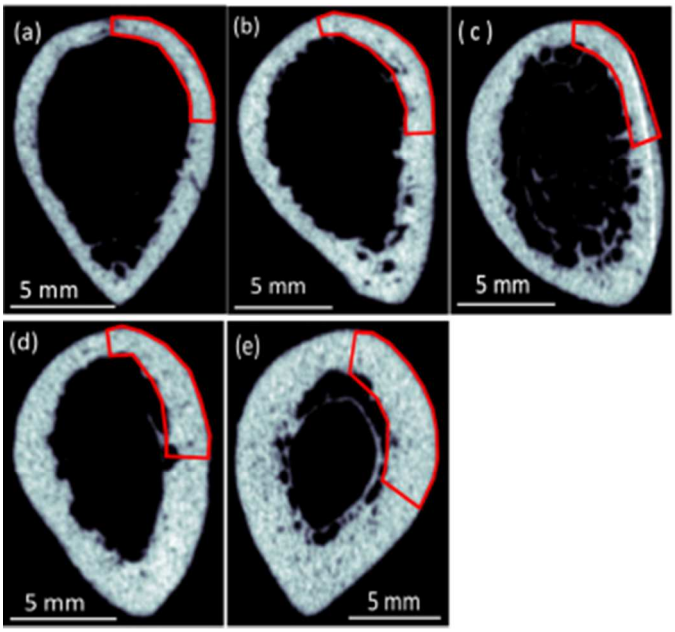

Fig 2: Transverse bone cross-sections obtained from HrpQCT meaurements. The red (color online) area indicates the region of interest for thickness assessment

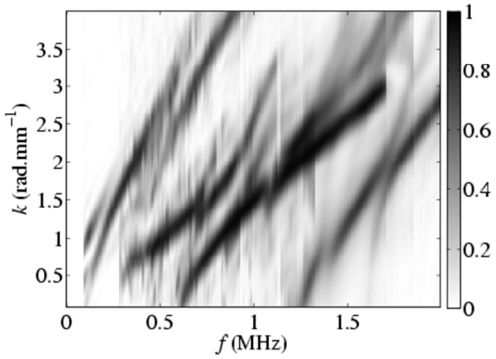

Fig 3: Norm function (frequency f, wavenumber k) for the 1.3 mm thick plate

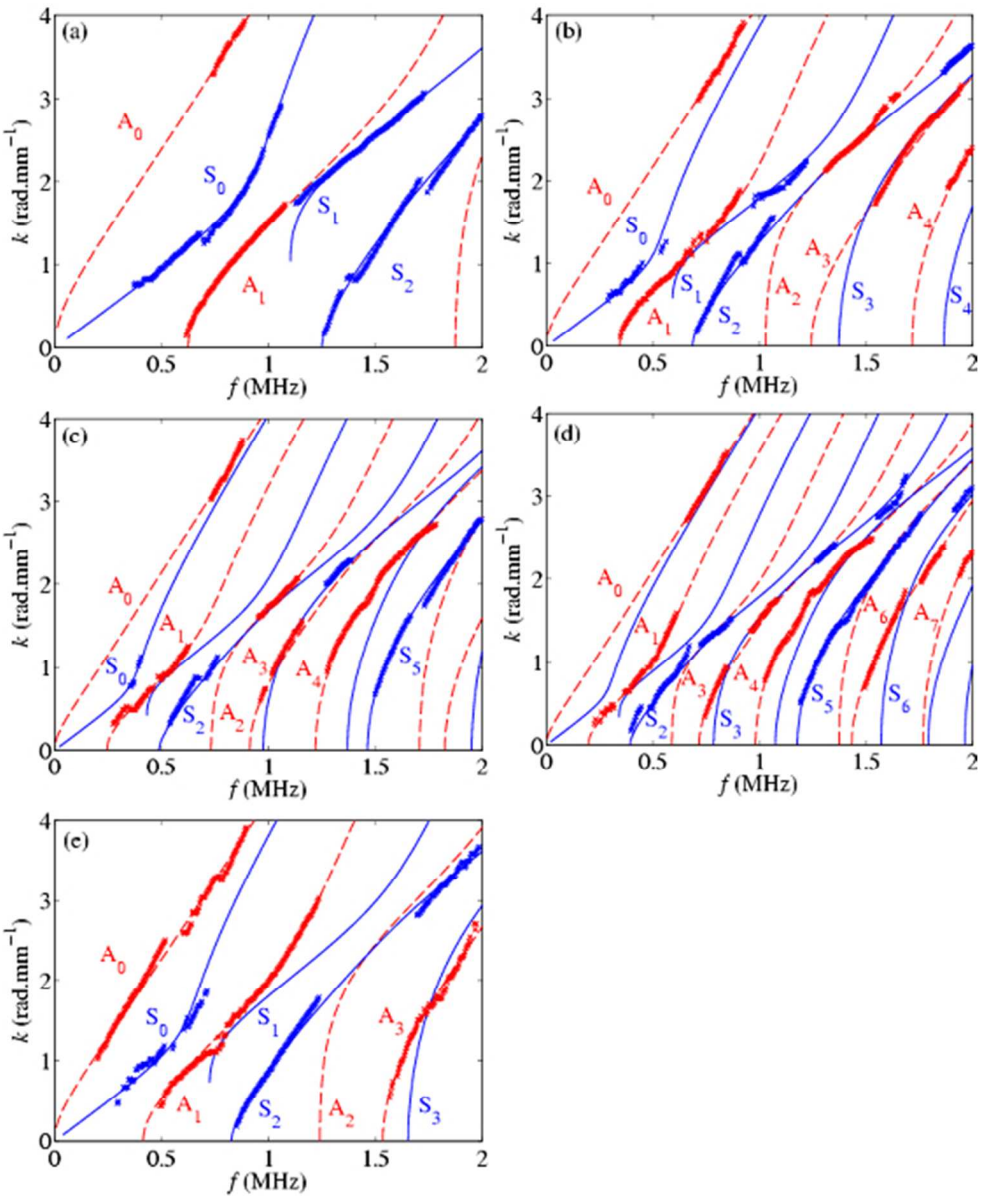

Fig. 4: (Color online). Plates and tube samples. Superposition of one measurement (crosses) and the best fit computed with the optimized parameters (lines) for the (a) 1.3 mm, (b) 2.30 mm, (c) 3.35 mm, (d) 4.15 mm-thick plates and (e) 2 mm-thick tube
147x181mm (96 x 96 DPI)

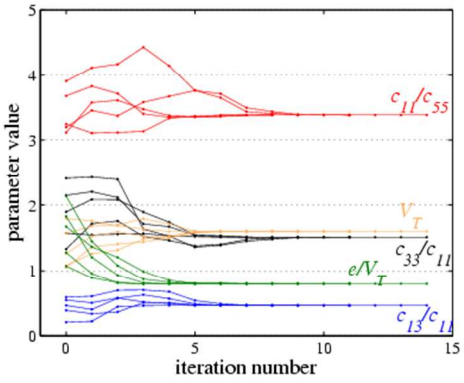

Fig. 5: (Color online). Plates and tube samples. Evolution of the value of the parameters during iterative process of minimization. Five sets of random initial values are considered.

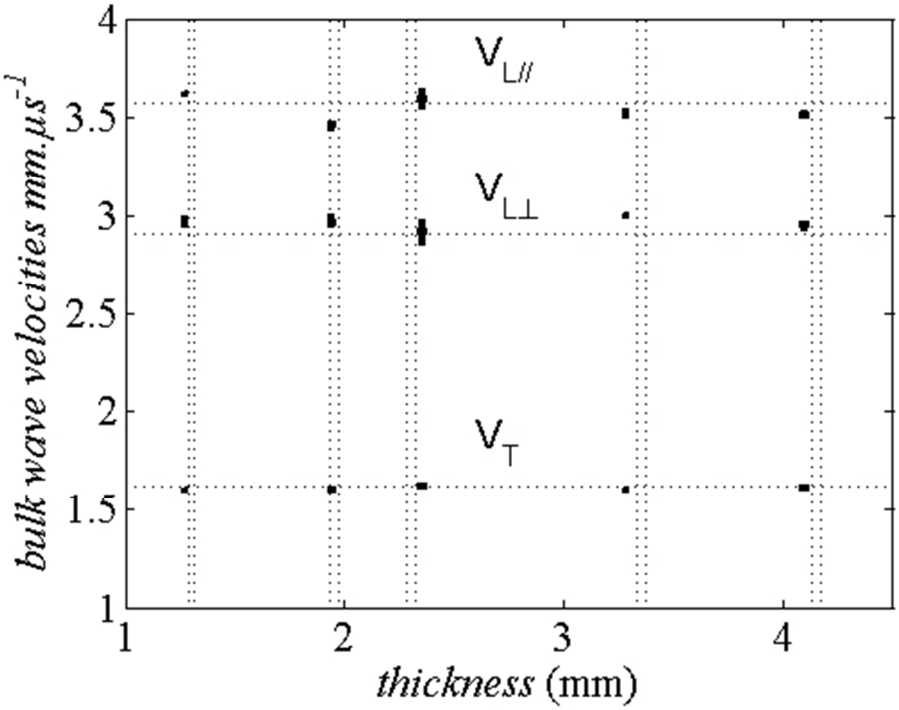

Fig. 6: Plates and tube samples. Estimated bulk wave velocities in x1 and x3 directions as function of the estimated thickness (bars). The width and height of the bars indicate the variability of the estimations over 30 meausrements (3 repositionings x 10 repetitive measurements). Horizontal dotted curves indicate reference velocities as given in Table 1. Vertical dotted lines indicate reference thickness as given in Table 2.
148x111mm (96 x 96 DPI)

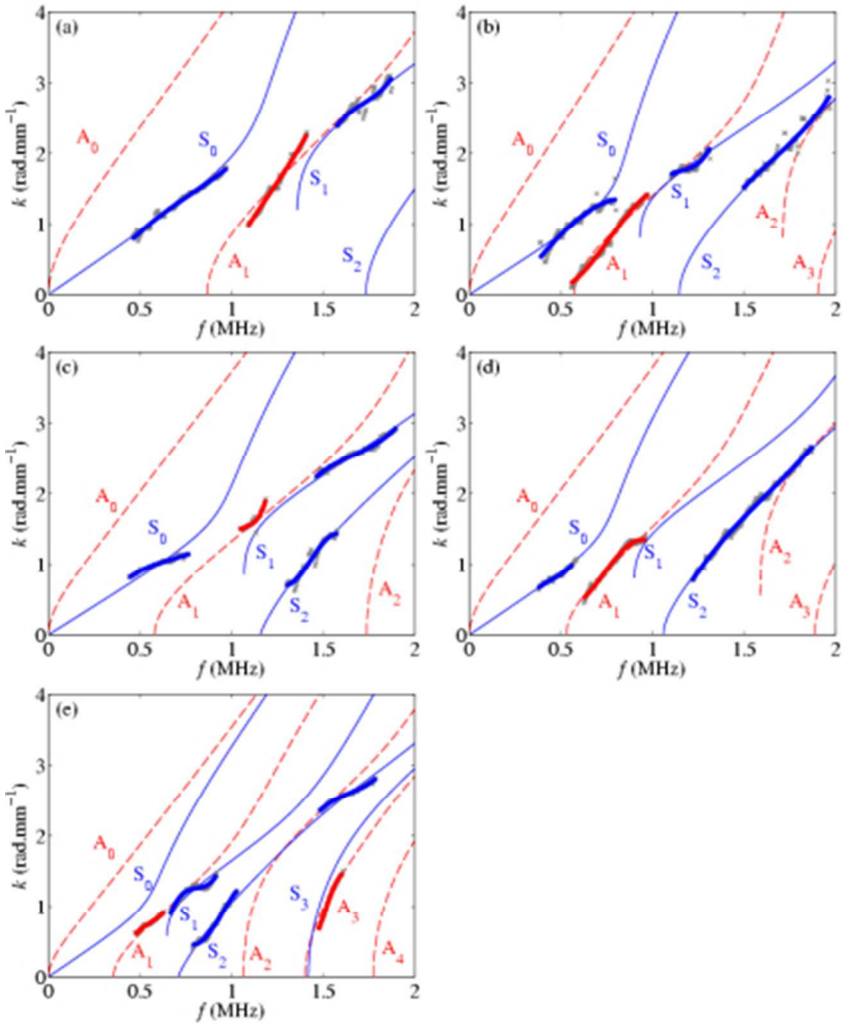

Fig. 7: Bone specimens. Superposition of one measurement (crosses) and the best fit computed with the optimized parameters for each of the five bone samples.